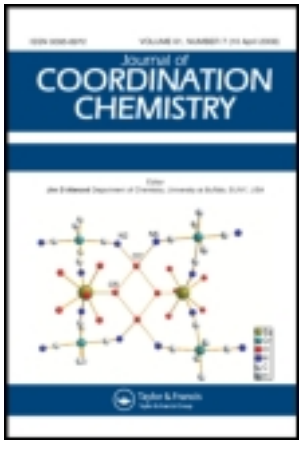

Journal of Coordination Chemistry
Publication details, including instructions for authors and subscription information:
http://www.tandfonline.com/loi/gcoo20

Four Zn(II)/Cd(II) coordination polymers derived from isomeric benzenedicarboxylates and 1,6-bis(triazol)hexane ligand: synthesis, crystal structure, and luminescent properties

Peng Zhang [a b], Dong-Sheng Li [a b], Jun Zhao [a], Ya-Pan Wu [a b], Cai Li [a], Kun Zou [a] & Jack Y. Lu [c]

[a] College of Mechanical and Material Engineering, Hubei Key Laboratory of Natural Products Research and Development, China Three Gorges University, Yichang 443002, China

[b] College of Chemistry and Chemical Engineering, Shaanxi Key Laboratory of Chemical Reaction Engineering, Yan'an University, Yan'an 716000, China

[c] Department of Chemistry, University of Houstons-Clear Lake, Houston, Texas 77058, USA

Published online: 05 Jul 2011.

To cite this article: Peng Zhang, Dong-Sheng Li, Jun Zhao, Ya-Pan Wu, Cai Li, Kun Zou & Jack Y. Lu (2011) Four Zn(II)/Cd(II) coordination polymers derived from isomeric benzenedicarboxylates and 1,6-bis(triazol)hexane ligand: synthesis, crystal structure, and luminescent properties, Journal of Coordination Chemistry, 64:13, 2329-2341, DOI: 10.1080/00958972.2011.597052

To link to this article: http://dx.doi.org/10.1080/00958972.2011.597052

Journal of Coordination Chemistry
Vol. 64, No. 13, 10 July 2011, 2329–2341

Four Zn(II)/Cd(II) coordination polymers derived from isomeric benzenedicarboxylates and 1,6-bis(triazol)hexane ligand: synthesis, crystal structure, and luminescent properties

PENG ZHANG†‡, DONG-SHENG LI*†‡, JUN ZHAO†, YA-PAN WU†‡, CAI LI†, KUN ZOU† and JACK Y. LU*§

†College of Mechanical and Material Engineering, Hubei Key Laboratory of Natural Products Research and Development, China Three Gorges University, Yichang 443002, China
‡College of Chemistry and Chemical Engineering, Shaanxi Key Laboratory of Chemical Reaction Engineering, Yan'an University, Yan'an 716000, China
§Department of Chemistry, University of Houstons-Clear Lake, Houston, Texas 77058, USA

(*Received 29 March 2011; in final form 6 June 2011*)

Four coordination polymers, $[Zn(o\text{-bdc})(bth)_{0.5}(H_2O)]_n$ (**1**), $[Cd(o\text{-bdc})(bth)_{0.5}(H_2O)]_n$ (**2**), $[Zn(m\text{-bdc})(bth)]_n$ (**3**), and $[Cd(p\text{-bdc})(bth)\cdot(H_2O)_2]_n$ (**4**) (where *o*-bdc = 1,2-benzenedicarboxylate, *m*-bdc = 1,3-benzenedicarboxylate, *p*-bdc = 1,4-benzenedicarboxylate, and bth = 1,6-bis(triazol)hexane), have been hydrothermally synthesized and structurally characterized. Both **1** and **2** are isostructural, featuring two binodal architectures: $(6^3)(6^5{\cdot}8)$ topology in terms of *o*-bdc and Zn^{II}/Cd^{II} as three- and four-connected nodes. Complex **3** shows a 2-D (4,4) network with the Zn···Zn···Zn angle of 57.84°, whereas **4** exhibits planar 2-D (4,4) network. These 2-D networks of **3** and **4** are extended by supramolecular interactions, such as $CH\cdots\pi/\pi$–π stacking and hydrogen-bonding into 3-D architecture. A structural comparison of these complexes demonstrates that the dicarboxylate building blocks with different dispositions of the carboxyl site play a key role in governing the coordination motifs as well as 3-D supramolecular lattices. Solid-state properties such as photoluminescence and thermal stabilities of **1**–**4** have also been studied.

Keywords: Zn^{II}/Cd^{II}-complexes; Isomeric benzenedicarboxylate; Crystal structure; Fluorescence

1. Introduction

Exploration of synthesis and properties of coordination polymers is of interest from chemists and material scientists for functional materials and fascinating structures [1]. However, control or predetermination of the final structures of the hybrid complexes remains challenging, because the molecular architectures of coordination polymers are

*Corresponding authors. Email: lidongsheng1@126.com; Lu@uhcl.edu

Journal of Coordination Chemistry
ISSN 0095-8972 print/ISSN 1029-0389 online
DOI: 10.1080/00958972.2011.597052

affected by coordination geometry of the metal ions, the nature of organic ligands, the choice of secondary ligand, reaction temperature, the counterions, the solvent system, pH, the metal-to-ligand ratio, and the method of crystallization [2]. Among many influential factors, bridging ligands, which contain adjustable flexibility and connectivity, play a crucial role in the construction and structural configuration of the final network [3].

Benzene-polycarboxylates are widely used in the formulation of functional materials because of their diverse coordination modes and bridging abilities as well as being readily functionalized at different sites [4]; benzenedicarboxylate, benzenetricarboxylate, and benzenetetracarboxylate are outstanding examples [5]. Polydentate aromatic nitrogen heterocycles with five-membered rings (azoles), especially for imidazoles and triazoles bearing alkyl spacers, are good N-donors, and the flexible spacers allow the ligands to bend and rotate to meet the steric requirement for metal binding [6]. Previous studies show that the combination of these polyazoles and aromatic polycarboxylates can result in novel topologies, magnetic, and luminescence properties [7]. A number of beautiful MOFs of ingenious design based on flexible bis(imidazole) ligands and benzenedicarboxylates (bdc, 1,2-bdc(*o*-bdc), 1,3-bdc(*m*-bdc), 1,4-bdc(*p*-bdc)) have been reported [8]. However, systematic studies on the three isomers of H_2bdc and bis(triazole) ligands in the construction of coordination polymers are rare. We used the three isomers of H_2bdc as bridging ligands and 1,6-bis(triazol)hexane as an auxiliary ligand (scheme 1) to construct d^{10} transition metal complexes, aiming to induce the evolution of new structures, or to obtain desirable luminescent complexes. Herein, we report four new 2-D/3-D d^{10} coordination polymers, $[Zn(o\text{-bdc})(bth)_{0.5}(H_2O)]_n$ (**1**), $[Cd(o\text{-bdc})(bth)_{0.5}(H_2O]]_n$ (**2**), $[Zn(m\text{-bdc})(bth)]_n$ (**3**), and $[Cd(p\text{-bdc})(bth)(H_2O)_2]_n$ (**4**). Their crystal structures and luminescent properties, along with the systematic investigation of the modulated effect of H_2bdc ligand on the ultimate framework, are presented and discussed.

2. Experimental

2.1. *Materials and general methods*

All commercially available solvents and reagents for synthesis and analysis were of reagent grade and used as received. C, H, and N elemental analyses were performed on a Perkin-Elmer 2400 CHN elemental analyzer. Infrared (IR) spectra as KBr pellets were

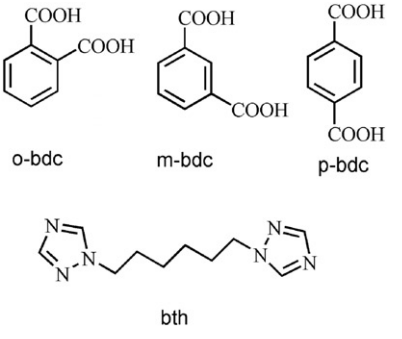

Scheme 1. Structures and abbreviations of the ligands.

recorded on a Thermo Nicolet Nexus670 spectrophotometer from 400 to 4000 cm^{-1}. Powder X-ray diffraction (PXRD) patterns were taken on a Rigaku D/max-2500 diffractometer (Cu-Kα radiation, $\lambda = 1.5406$ Å), with a scan speed of 2° per min and a step size of 0.02° in 2θ. The calculated PXRD patterns were simulated using the single-crystal XRD data. Thermogravimetric analyses (TGA) were performed on a Netzsch STA 449C microanalyzer under air at a heating rate of 10°C min^{-1}. Solid-state fluorescence spectra were recorded on a Hitachi F-4500 fluorescence spectrophotometer at room temperature.

2.2. *Synthesis*

2.2.1. Preparation of [Zn(*o*-bdc)(bth)$_{0.5}$(H_2O)]$_n$ (1). An H_2O/CH_3OH solution (8.0 mL) containing $Zn(NO_3)_2 \cdot 6H_2O$ (20 mg, 0.1 mmol), *o*-H_2bdc (16.6 mg, 0.1 mmol), bth (22 mg, 0.05 mmol), and NaOH (0.4 mmol) was sealed in a 23 mL Teflon-lined autoclave, heated at 140°C for 3 days and then cooled to room temperature at 5°C min^{-1}. Colorless block single crystals of **1** were obtained (yield: 59% based on zinc). Anal. Calcd for $C_{13}H_{14}N_3O_5Zn$ (%): C, 43.65; H, 3.95; N, 11.75. Found (%): C, 44.39; H, 4.95; N, 11.32. IR (cm^{-1}, KBr): 3400 (w), 3118 (w), 2941 (w), 1610 (vs), 1561 (vs), 1539 (s), 1490 (m), 1421 (m), 1389 (vs), 1280 (m), 1138 (m), 997 (m), 871 (w), 837 (w), 763 (s), 707 (w), 656 (vs).

2.2.2. Preparation of [Cd(*o*-bdc)(bth)$_{0.5}$(H_2O)]$_n$ (2). A similar procedure to that of **1** was used, except that $Zn(NO_3)_2 \cdot 6H_2O$ was replaced by $Cd(NO_3)_2 \cdot 4H_2O$ (30.8 mg, 0.1 mmol). Colorless block single crystals of **2** were obtained (yield: 57% based on cadmium). Anal. Calcd for $C_{13}H_{14}CdN_3O_5$ (%): C, 38.58; H, 3.49; N, 10.38. Found (%): C, 38.82; H, 3.05; N, 10.57. IR (cm^{-1}, KBr): 3493 (w), 2826 (m), 1685 (s), 1611(m), 1420 (w), 1279 (s), 1163 (w), 924 (w), 831 (w), 725 (s), 690 (m), 671 (w).

2.2.3. Preparation of [Zn(*m*-bdc)(bth)]$_n$ (3). This complex was prepared in a similar procedure to that of **1** using *m*-H_2bdc (16.6 mg, 0.1 mmol) in place of *o*-H_2bdc. Block colorless crystals were obtained (yield: 56% based on zinc). Anal. Calcd for $C_{18}H_{20}N_6O_4Zn$ (%): C, 48.06; H, 4.48; N, 18.68. Found (%): C, 48.40; H, 4.61; N, 18.45. IR (cm^{-1}, KBr): 1619 (s), 1577 (m), 1531 (m), 1386 (m), 1338 (s), 1274 (m), 1133 (w), 999 (m), 831 (w), 759 (s), 724 (s), 678 (s), 663 (w).

2.2.4. Preparation of [Cd(*p*-bdc)(bth)$\cdot$(H_2O)$_2$]$_n$ (4). This complex was prepared in a similar procedure to that of **1** using *p*-H_2bdc (16.6 mg, 0.1 mmol) in place of *o*-H_2bdc and $Cd(NO_3)_2 \cdot 6H_2O$ (30.8 mg, 0.1 mmol) in place of $Zn(NO_3)_2 \cdot 6H_2O$. Colorless block single crystals of **4** were obtained (yield: 58% based on cadmium). Anal. Calcd for $C_{18}H_{24}CdN_6O_6$ (%): C, 40.57; H, 4.54; N, 15.77. Found (%): C, 40.35; H, 4.61; N, 15.91%. IR (cm^{-1}, KBr): 3450 (w), 1685 (m), 1611 (s), 1581 (m), 1486 (m), 1431 (w), 1420 (m), 1278 (s), 1163 (m), 1099 (m), 924 (w), 831 (w), 725 (m), 724 (m), 690 (w), 666 (w).

2.3. *X-ray crystallography*

Single-crystal XRD measurements for **1**–**4** were carried out on a Bruker APEX II diffractometer equipped with a graphite-crystal monochromator situated in the incident

Table 1. Crystal data and structure refinement information for **1–4**.

Complex	**1**	**2**	**3**	**4**
Empirical formula	$C_{13}H_{14}N_3O_5Zn$	$C_{13}H_{14}CdN_3O_5$	$C_{18}H_{20}N_6O_4Zn$	$C_{18}H_{24}CdN_6O_6$
Formula weight	357.64	404.67	449.77	532.83
Crystal system	Monoclinic	Monoclinic	Orthorhombic	Triclinic
Space group	$P2_1/c$	$P2_1/n$	*Pnma*	$P\bar{1}$
Unit cell dimensions (Å, °)				
a	6.130(2)	6.2452(12)	13.2702(13)	5.5677(3)
b	9.252(3)	8.9599(18)	15.4492(15)	8.9869(5)
c	25.154(8)	26.138(5)	9.5815(9)	10.6725(6)
β	96.825(4)	96.06(3)	90	84.7960(10)
Volume (Å^3), Z	1416.6(8), 4	1454.4(5), 4	1964.3(3), 4	506.05(5), 1
Temperature (K)	293(2)	298(2)	298(2)	293(2)
Calculated density ρ_{calcd} (g cm^{-3})	1.677	1.848	1.521	1.748
$F(000)$	732	804	928	270
Reflections collected	7177	17,359	12,299	6327
Reflections unique	2464	3607	1798	2566
Goodness-of-fit	1.026	1.093	1.035	1.019
R_{int}	0.0282	0.0683	0.0299	0.0159
R_1, wR_2 [$I > 2\sigma(I)$]	0.0371, 0.0975	0.0336, 0.0994	0.0569, 0.1365	0.0190, 0.0521
R_1, wR_2 (all data)	0.0449, 0.1028	0.0349, 0.1006	0.0600, 0.1390	0.0190, 0.0522

$R_1 = \sum||F_o| - |F_c||/\sum|F_o|$. $wR_2 = \{\sum[w(F_c^2 - F_c^2)^2]/\sum[w(F_c^2)^2]\}^{1/2}$.

beam for data collection. Determinations of unit cell parameters and data collections were performed with Mo-Kα radiation ($\lambda = 0.71073$ Å). Semi-empirical absorption corrections were applied using SADABS. All structures were solved by direct methods using SHELXS of SHELXTL package and refined with SHELXL [9]. Metal ions were found from *E*-maps, and other non-hydrogen atoms were located by successive difference Fourier synthesis. The final refinement was performed by full-matrix least-squares with anisotropic thermal parameters for non-hydrogen atoms on F^2. The hydrogens of organic ligands were located theoretically and refined with fixed thermal factors. The water hydrogens were located from difference maps and refined with isotropic temperature factors. Crystallographic data and experimental details for the structural analyses are summarized in table 1 and selected bond parameters in table 2.

3. Results and discussion

3.1. *Preparation and IR spectra of 1–4*

Complexes **1**–**4** were prepared under similar hydrothermal conditions in moderate yields. All complexes are air stable and were characterized by elemental analyses and IR spectra. In the IR spectra of **1**, **2**, and **4**, a broad band centered at ~3400 cm^{-1} indicates O–H stretching of water. For **1**–**4**, the IR spectra display characteristic bands of carboxylate at ~1610 and ~1535 cm^{-1} for $\nu_{asym(C-O)}$, ~1380 cm^{-1} for $\nu_{sym(C-O)}$; the $\Delta\nu$ values ($\nu_{asym} - \nu_{sym}$) are 221 and 150 cm^{-1} for **1**, 255 cm^{-1} for **2**, 233 and 145 cm^{-1} for **3**, 161 and 191 cm^{-1} for **4**, respectively. The splitting of $\nu_{asym(C-O)}$ indicates different coordination modes of carboxylate, being in agreement with their crystal structures. The absence of characteristic bands at 1730–1690 cm^{-1} for carboxyl indicates complete deprotonation of the ligands in all these complexes. The carboxylate IR adsorption is very complicated due to its coordination diversity with metal ions.

Table 2. Selected bond lengths (Å) and angles (°) for **1**[a]–**4**[d].

1[a]			
Zn1–O2#1	1.978(2)	Zn1–O4#2	2.071(3)
Zn1–O1	2.016(2)	Zn1–O5	2.283(3)
O2–Zn1#3	1.978(2)	O4–Zn1#4	2.071(3)
Zn1–N1	2.035(3)		
O2#1–Zn1–O1	110.02(9)	O2#1–Zn1–N1	127.15(11)
O1–Zn1–N1	121.23(10)	O2#1–Zn1–O4#2	101.72(10)
O1–Zn1–O4#2	93.36(10)	N1–Zn1–O4#2	87.99(11)
O2#1–Zn1–O5	85.96(10)	O1–Zn1–O5	80.83(10)
N1–Zn1–O5	89.93(11)	O4#2–Zn1–O5	171.67(10)
2[b]			
Cd1–O1	2.239(2)	Cd1–O4#1	2.253(3)
Cd1–O2#2	2.260(2)	Cd1–O5	2.358(2)
Cd1–O2	2.641(2)	O4–Cd1#3	2.253(3)
O2–Cd1#4	2.260(2)	Cd1–N1	2.262(2)
O1–Cd1–O4#1	103.34(10)	O1–Cd1–N1	137.11(9)
O4#1–Cd1–N1	83.37(9)	O1–Cd1–O2#2	109.30(8)
O4#1–Cd1–O2#2	94.24(9)	N1–Cd1–O2#2	112.39(9)
O1–Cd1–O5	88.55(9)	O4#1–Cd1–O5	167.84(10)
N1–Cd1–O5	89.65(10)	O2#2–Cd1–O5	79.19(7)
O1–Cd1–O2	52.75(7)	O4#1–Cd1–O2	112.11(9)
N1–Cd1–O2	85.18(8)	O2#2–Cd1–O2	150.25(2)
O5–Cd1–O2	77.04(7)	–	–
3[c]			
Zn1–O4#1	1.921(4)	Zn1–O1	1.964(4)
O4–Zn1#3	1.921(4)	Zn1–N1	2.022(4)
Zn1–N1#2	2.022(3)	–	–
O4#1–Zn1–O1	117.19(17)	O4#1–Zn1–N1	117.91(11)
O1–Zn1–N1	96.02(12)	O4#1–Zn1–N1#2	117.91(11)
O1–Zn1–N1#2	96.02(12)	N1–Zn1–N1#2	107.8(2)
4[d]			
Cd1–O1	2.2976(11)	Cd1–O1#1	2.2976(11)
Cd1–O3	2.3365(13)	Cd1–O3#1	2.3365(13)
Cd1–N10	2.3333(14)	Cd1–N10#1	2.3333(14)
O1–Cd1–O1#1	180.0	O1–Cd1–N10	85.20(5)
O1#1–Cd1–N10	94.80(5)	O1–Cd1–N10#1	94.80(5)
O1#1–Cd1–N10#1	85.20(5)	N10–Cd1–N10#1	180.00(6)
O1–Cd1–O3	89.72(5)	O1#1–Cd1–O3	90.28(5)
N10–Cd1–O3	89.31(5)	N10#1–Cd1–O3	90.69(5)
O1–Cd1–O3#1	90.28(5)	O1#1–Cd1–O3#1	89.72(5)
N10–Cd1–O3#1	90.69(5)	N10#1–Cd1–O3#1	89.31(5)
O3–Cd1–O3#1	180.00(7)	–	–

Symmetry codes: **a**: #1, $-x$, $-0.5+y$, $0.5-z$; #2, $1+x$, y, z; #3, $-x$, $0.5+y$, $0.5-z$; #4, $-1+x$, y, z. **b**: #1, $1.5-x$, $0.5+y$, $0.5-z$; #2, $0.5-x$, $0.5+y$, $0.5-z$; #3, $1.5-x$, $-0.5+y$, $0.5-z$; #4, $0.5-x$, $-0.5+y$, $0.5-z$. **c**: #1, x, y, $1+z$; #2, x, $0.5-y$, z; #3, x, y, $-1+z$; **d**: #1, $2-x$, $1-y$, $-z$.

3.2. *Structural description of 1–4*

3.2.1. $[Zn(o\text{-bdc})(bth)_{0.5}(H_2O)]_n$ (1) and $[Cd(o\text{-bdc})(bth)_{0.5}(H_2O)]_n$ (2). Single-crystal XRD analysis reveals that **1** and **2** are isostructural, except that one bth in **1** is replaced by disordered bth in **2**. Therefore, only the crystal structure of **1** is discussed herein. The asymmetric unit of **1** contains a Zn^{II}, one *o*-bdc anion, half bth, and a coordinated water molecule. As shown in figure 1(a), each Zn is coordinated by one nitrogen of one bridging bth ligand, four oxygens from three individual *o*-bdc anions, and one water molecule, resulting in an elongated trigonalbipyramid {ZnNO4} configuration.

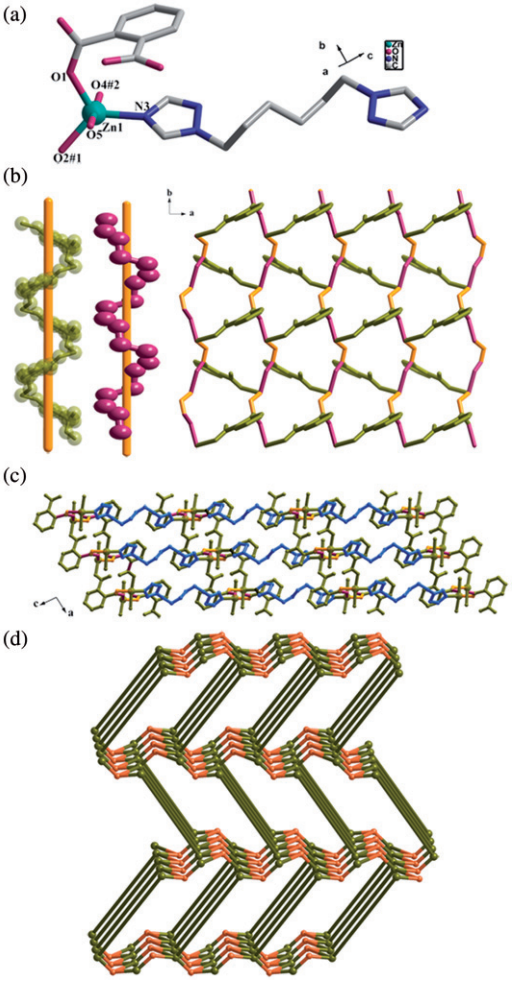

Figure 1. (a) Coordination environment of zinc in **1**. (b) A unique 2-D layer is formed by left helical chains (purple) and right ones (dark yellow) with zincs functioning as hinges and light orange representing common edges. (c) The 3-D herringbonelike structure. (d) Schematic representation of (3,4)-connected (6^3) ($6^5{\cdot}8$) topology (Zn are indicated by dark yellow balls and the *o*-bdc linkers are simplified as orange balls).

The Zn–O distances fall in the range 1.978(2)–2.283(3) Å and the Zn–N bond length is 2.035(3) Å, consistent with the corresponding values reported [10].

In **1**, the carboxyl groups of *o*-bdc display two coordination modes, μ_2–η^1:η^1 (C_7OO^-) and μ_1–η^1 (C_8OO^-), which play an important role in forming distinct hetero-chiral helical chains. First, the μ_2-carboxylate (O1 and O2) group alternately connects Zn^{II} cations to yield a left-hand helix along the *c*-axis, in which the Zn···Zn distance is 4.8776 Å. Second, Zn^{II} centers are linked by μ_2-carboxylate (O1) and μ_1-carboxylate (O4) groups into a right-helix along the (001) plane, with Zn···Zn distance 9.253 Å. As a result, with zinc functioning as hinges, these two types of helices are alternately attached to build a unique 2-D layer in the *ab* plane (figure 1b). In **1**, each bth is a linker and exhibiting the conformation of TGGGT (T = *trans*, G = gauche) (table 3 and table S1). These helical layers are pillared by bth to yield a 3-D herringbonelike architecture (figure 1c).

Table 3. Conformational parameters of bth in **1**, **3**, and **4**.

Complex	**1**	**3**	**4**
Conformation of bth	TGGGT	GGGGG	GGGGG
N···N	N3···N3A	N2···N2A	N7···N7A
Distance	9.287	8.686	8.790
M···M	Zn1···Zn1A	Zn1···Zn1A	Cd1···Cd1A
Distance	15.371	15.973	15.866
Dihedral angle of two triazole rings	0	0	0

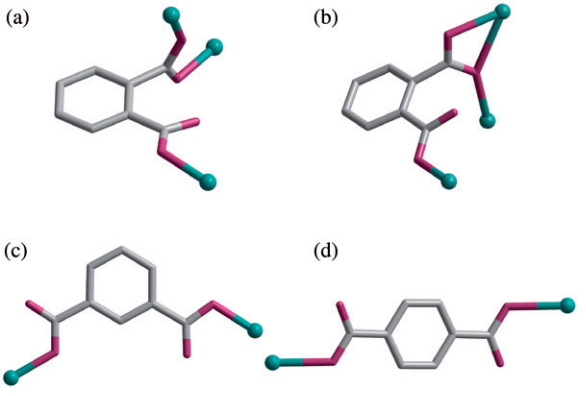

Scheme 2. Coordination modes of aromatic dicarboxylates.

Topological analysis reveals **1** is a (3,4)connected net with (6^3) $(6^5{\cdot}8)$ topology, if the *o*-bdc and Zn are treated as threeconnected and fourconnected nodes, respectively (figure 1d). There are hexagons (the smallest circuits) around each *o*-bdc linker. Similarly, the shortest rings of each fourconnected node are hexagons and octagons. The long Schläfli vertical symbol is $6{\cdot}6{\cdot}6_2$ for the 3-c node and $6{\cdot}6{\cdot}6{\cdot}6{\cdot}6{\cdot}8_2$ for the 4-c node, giving the net symbol $(6{\cdot}6{\cdot}6_2)$ $(6{\cdot}6{\cdot}6{\cdot}6{\cdot}6{\cdot}8_2)$. In **1**, *o*-bdc as the three-connected node connect three metal nodes exhibiting common (3,4)-connected nets. While there exist many examples of (3,4)-connected nets, the majority are involved in boracite, Pt_3O_4, and cubic-C_3N_4 [11].

In **1** and **2**, although *o*-bdc's adopt μ_3-bridging mode, they show different coordination geometry: for **1**, *o*-bdc is a μ_3–$\eta^1:\eta^1:\eta^1$ bridging ligand linking three Zn^{II}'s with one μ_2–$\eta^1:\eta^1$ carboxylate and one μ_1–η^1 carboxylate; however, for **2**, *o*-bdc is a μ_3–$\eta^1:\eta^2:\eta^1$ bridging ligand coupling three Cd^{II}'s *via* μ_2–$\eta^1:\eta^2$ carboxylate and μ_1–η^1 carboxylate groups (scheme 2). This difference may be mainly attributed to the different coordinations of the metal centers (five-coordinate for Zn^{II} of **1** and six-coordinate for Cd^{II} of **2**).

3.2.2. [Zn(*m*-bdc)(bth)]$_n$ (3). As illustrated in figure 2(a), the asymmetric unit of **3** comprises a Zn^{II}, one *m*-bdc anion, and one bth; each Zn is surrounded by two oxygens from one *m*-bdc with bis(monodentate) coordination and two nitrogens from different bth ligands adopting TGGGT (T = *trans*, G = gauche) bridging conformation, showing a slightly distorted tetrahedral {ZnO2N2} geometry. The Zn–O/N bonds are in the

range 1.922(4)–2.022(4) Å, which are within the expected range [12]. In **3**, the Zn^{II} centers are connected by bth to afford a 1-D zigzag chain along the crystallographic *b* direction (figure 2b), in which the distance of adjacent Zn^{II} ions is 15.973 Å and the Zn···Zn···Zn angle is 57.84°. The 1-D zigzag chains are interlinked by *m*-bdc anions, constituting waved 2-D (4,4) networks (figure 2c). Further investigation of the crystal packing of **3** suggests that there are two kinds of supramolecular interactions (C–H···O and CH–π) between adjacent 2-D layers. Among them, the C–H···O hydrogen bonding from the uncoordinated carboxyl groups (O2 and O3) of different *o*-bdc anions in the adjacent layer and carbons of triazol (C9) and phenyl (C7) rings in

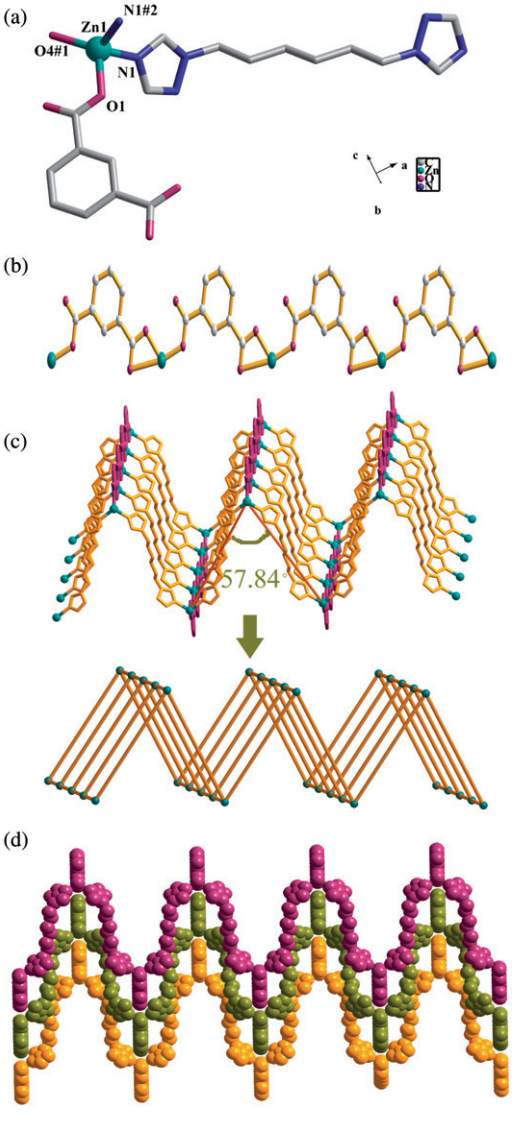

Figure 2. (a) Coordination environment of zinc in **3**. View of (b) 1-D zigzag chain, (c) waved layer and simplified models applied in the topological analysis, and (d) 3-D supramolecular structure.

different layers (C–H···O: C9···O2, 3.184 Å and 168.38°; C7···O3, 3.326 Å and 168.12°); CH–π stacking arises from phenyl (C5) and triazol rings in contiguous layers (CH–π: 3.539 Å and 135.39°). Through these interactions, the waved 2-D (4,4) networks are extended to 3-D in an embedding fashion (figure 2d).

3.2.3. [Cd(*p*-bdc)(bth)·$(H_2O)_2]_n$ (4). The asymmetric unit of **4** consists of a Cd^{II}, one *p*-bdc anion, one bth, plus two coordinated water molecules. Each Cd^{II} is six-coordinate to two nitrogens from different bth ligands and four oxygens from two μ_2-*p*-bdc anions and two coordinated water molecules, affording a distorted octahedral {CdN2O4} geometry (figure 3a). The $Cd–O_{carboxyl}$ distance (2.298(1) Å) is slightly shorter than $Cd–O_{water}$ (2.337(1) Å) and Cd–N (2.333(1) Å) bond lengths [13].

In **4**, the Cd^{II} centers are interlinked by μ_2-*p*-bdc with bis(monodentate) coordination and bth adopting GGGGG conformation into planar 2-D (4,4) networks with the adjacent Cd···Cd distances of 11.581 and 15.866 Å, respectively (figure 3b). These 2-D sheets, evidently, are readily involved in secondary interactions such as hydrogen bonding and π–π stacking, and thus, can be regarded as supramolecular building blocks. Strong O–H···O hydrogen bonding occurs between coordinated

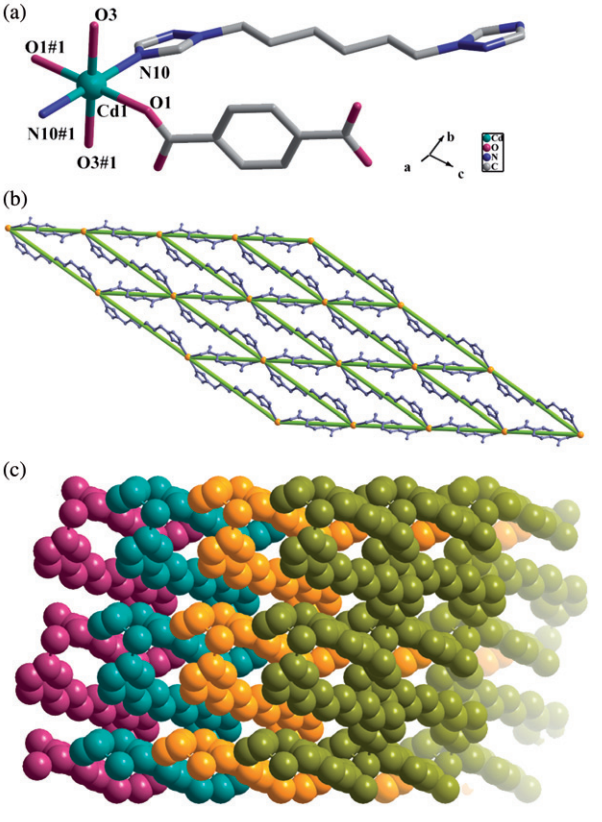

Figure 3. (a) Coordination environment of cadmium in **4**. View of (b) planar 2-D (4,4) network, and (c) the 3-D supramolecular structure.

water (O3) and carboxylates (O1 for the neighboring sheets and O2 for same sheet), whereas CH $\cdots$ π/π–π stacking interactions resulting from triazol rings of bth exist from different sheets/within the sheet (table S2). As a corollary, these 2-D sheets are assembled into a 3-D supramolecular architecture (figure 3c).

3.3. *Structural comparisons of* 1–4

In all structures, μ_2-bth shows two types of coordination conformation: TGGGT for **1** and GGGGG for **3** and **4** (bth is disordered in **2**). However, the corresponding N $\cdots$ N distance between N donors, the M $\cdots$ M separation, and the dihedral angles of two triazol rings are similar in all complexes (table 3 and table S1); bth ligands uniformly behave as bidentate spacers to connect Zn^{II}/Cd^{II} centers in the resulting networks of **1**–**4**. Thus, the structural diversity of **1**–**4** should be mainly attributed to the positional isomeric effect of bdc and/or the metal ions with different coordination tendencies. For **1** and **2**, the *o*-bdc anions adopt μ_3-bridging coordination linking Zn^{II}/Cd^{II} centers into 2-D helical layers. For **3** and **4**, Zn^{II}/Cd^{II} are connected by μ_2-*m*-bdc/μ_2-*p*-bdc anions both bis(monodentate) into a 1-D chain. Through connection of bth ligands, these 2-D layers (**1** and **2**) or 1-D chains (**3** and **4**) are pillared to 3-D coordination framework (**1** and **2**) and 2-D coordination nets [waved (4,4) net for **3** (four-coordinate Zn^{II}) and planar (4,4) net for **4** (six-coordinate Cd^{II}), indicating metal-directed assembly]. Secondary interactions are also critical to construct the overall supramolecular lattices of **3** and **4**, in which significant stacking and/or hydrogen-bonding contacts are observed.

1-D/2-D/3-D Zn^{II}/Cd^{II}-coordination polymers have been achieved on the basis of the choice benzenedicarboxylate and N-donor ligands [14, 15]. In these complexes, the benzenedicarboxylic acids always exhibit rich coordination modes owing to their rigidity and polycarboxylates, and play an important role in governing the structures of such crystalline materials. However, systems with chelating N,N′-donors serving as terminal ligands, such as 2,2′-bipyridine, 1,10-phenanthroline, or their derivatives, reduce the available metal ion binding sites to interdict polymer growth in other directions, resulting in low dimensionality structures [14]; different bridging N-donor ligands, such as 4,4′-bipyridine-like ligands, may further extend the coordination array, leading to 2-D/3-D frameworks [15]. Compared with our work, if auxiliary N-donors play a bridging role, the resulting framework will be mainly mediated by H_2bdc isomers and/or different coordinated metals. Thus, the structural diversity of such systems is attributed to the synergetic effect of benzenedicarboxylate, auxiliary ligands, and metal centers used in the assembly process.

3.4. *TGA and PXRD*

To confirm the phase purity of the bulk materials, the PXRD experiments were carried out for **1**–**4** (figure S1). Although the experimental patterns have a few unindexed diffraction peaks and some are slightly broadened in comparison to those simulated from the single-crystal data, it can still be regarded that the bulk as-synthesized materials represent **1**–**4**.

Thermal stabilities of **1**–**4** have been investigated by TGA, and the TGA curves are shown in figure S2. The TGA curves of **1** and **2** are similar due to their isostructural

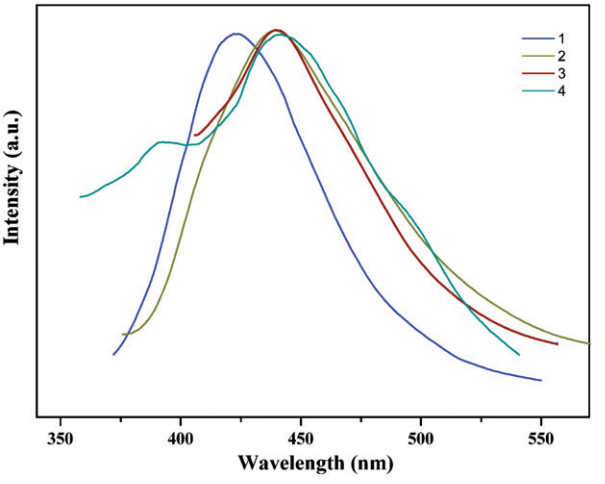

Figure 4. The solid-state emission spectra of **1–4** at room temperature.

nature. The first weight loss for **1** (4.7%) and for **2** (4.8%) indicates exclusion of coordinated water (Calcd: 5.0% and 4.5%). The residual solids show a series of consecutive weight losses from 274° to 529° for **1**, 216° to 507° for **2**. For **3**, there are no lattice and coordinated water and thus, pyrolysis starts at 287°C. For **4**, weight loss attributed to gradual release of coordinated water is observed from 30°C to 213°C (Obsd: 6.9% and Calcd: 6.7%). Further, decomposition occurs at 257°C. For **1–4**, the remaining weight indicates that the final residue is ZnO or CdO.

3.5. *Fluorescence properties*

Organic–inorganic coordination polymers, especially those with d^{10} metal centers, have been investigated for fluorescence and potential applications as fluorescence-emitting materials [16]. The solid-state photoluminescence spectra of **1–4** and free bth were measured at room temperature, and the results are given in figure 4. No clear luminescence was detected for bth, while the Zn^{II}/Cd^{II} complexes exhibit emissions at 423 nm for **1**, at 447 nm for **2**, at 447 nm for **3**, and at 388 and 448 nm for **4**. In comparison to free *o*/*m*/*p*-bdc [13, 17], the emission maxima of **1–4** are changed, assigned neither to metal-to-ligand charge transfer (MLCT) nor to ligand-to-metal transfer (LMCT), since the Zn^{II} and Cd^{II} ions are difficult to oxidize or reduce. Thus, they may be assigned to intraligand (π–π^*) fluorescent emission [15]. Different shifts for emission of **1–4** may result from coordination to the metal centers [15].

4. Conclusion

Four new Zn^{II}/Cd^{II} complexes were generated from mixed-ligand systems of three benzenedicarboxylate isomers and 1,6-bis(triazol)hexane. Structural comparisons among **1–4** indicate that the backbone of bdc plays an important role in governing

the structures of such crystalline materials, and bridging bth leads to the formation of 2-D/3-D coordination polymers. These results reveal the isomeric effect of the mixed-ligands in molecular tectonics of the metal–organic frameworks and provide new insights into its application in engineering such crystalline solids with desirable structures and properties. Further efforts on the design and preparation of coordination networks with other phenyl dicarboxylate tectons are underway in our lab.

Supplementary material

CCDC Nos 782963–782966 contain the supplementary crystallographic data for **1**–**4**. These data can be obtained free of charge from The Cambridge Crystallographic Data Centre *via* www.ccdc.cam.ac.uk/data_request/cif. Supplementary data associated with this article can be found in the section of supporting information.

Acknowledgments

This work was financially supported by the NSF of China (21073106, 20773104), NCET (NCET-06-0891), the IPHPEO (Z20091301, Q Q20101203), and the NSF of Hubei Provinces of China (2010CDB10707), and J.Y. Lu's support from Welch Foundation.

References

[1] (a) B. Moulton, M.J. Zaworotko. *Chem. Rev.*, **101**, 1629 (2001); (b) M.H. Zeng, Q.X. Wang, Y.X. Tan, S. Hu, H.X. Zhao, L.S. Long, M. Kurmoo. *J. Am. Chem. Soc.*, **132**, 2561 (2010); (c) A. Phan, C.J. Doonan, F.J. Uribe-Romo, C.B. Knobler, M. O'Keeffe, O.M. Yaghi. *Acc. Chem. Res.*, **43**, 58 (2009); (d) D.S. Li, Y.P. Wu, P. Zhang, M. Du, J. Zhao, C.P. Li. *Cryst. Growth Des.*, **10**, 2037 (2010).

[2] (a) L. Carlucci, G. Ciani, D.M. Proserpio, S. Rizzato. *New J. Chem.*, **27**, 483 (2003); (b) P.M. Forster, A.R. Burbank, C. Livage, G. Férey, A.K. Cheetham. *Chem. Commun.*, 368 (2004); (c) L.F. Ma, L.Y. Wang, M. Du, S.R. Batten. *Inorg. Chem.*, **49**, 365 (2010); (d) I.S. Lee, D. MokShin, Y.K. Chung. *Chem. Eur. J.*, **10**, 3158 (2004); (e) D.S. Li, X.J. Ke, J. Zhao, M. Du, K. Zou, Q.F. He, C. Li. *CrystEngComm*, **13**, 3335 (2011); (f) D.M. Shin, I.S. Lee, D. Cho, Y.K. Chung. *Inorg. Chem.*, **42**, 7722 (2003).

[3] (a) M.L. Zhang, D.S. Li, J.J. Wang, F. Fu, M. Du, K. Zou, X.M. Gao. *Dalton Trans.*, 5355 (2009); (b) N. Li, L. Gou, H.M. Hu, S.H. Chen, X.L. Chen, B.C. Wang, Q.R. Wu, M.L. Yang, G.L. Xue. *Inorg. Chim. Acta*, **362**, 3475 (2009).

[4] (a) J.Y. Lu. *Coord. Chem. Rev.*, **246**, 327 (2003); (b) M. Du, X.J. Zhao, J.H. Guo, S.R. Batte. *Chem. Commun.*, 4836 (2005).

[5] (a) G.P. Yang, Y.Y. Wang, W.H. Zhang, A.Y. Fu, R.T. Liu, E.K. Lermontova, Q.Z. Shi. *CrystEngComm.*, **12**, 1509 (2010); (b) L.F. Ma, C.P. Li, L.Y. Wang, M. Du. *Cryst. Growth Des.*, **10**, 2641 (2010); (c) J.J. Wang, L. Gou, H.M. Hu, Z.X. Han, D.S. Li, G.L. Xue, M.L. Yang, Q.Z. Shi. *Cryst. Growth Des.*, **7**, 1515 (2007).

[6] (a) S. Das, S. Pal. *J. Mol. Struct.*, **741**, 183 (2005); (b) J.G. Liu, S.Q. Zang, Z.F. Tian, Y.Z. LI, Y.Y. Xu, H.Z. Zhu, Q.J. Meng. *CrystEngComm.*, **9**, 915 (2007); (c) C.X. Meng, D.S. Li, J. Zhao, F. Fu, X.N. Zhang, L. Tang, Y.Y. Wang. *Inorg. Chem. Commun.*, **12**, 793 (2009); (d) M. Pan, X.L. Zheng, Y. Liu, W.S. Liu, C.Y. Su. *Dalton Trans.*, 2157 (2009); (e) X.J. Ke, D.S. Li, J. Zhao, C.X. Meng, X.N. Zhang, Q.F. He, C. Li, Y.Y. Wang. *Inorg. Chem. Commun.*, **13**, 484 (2010).

[7] (a) N. Liu, Y.Q. Wang, E.Q. Gao, Z.X. Chen, L.H. Weng. *CrystEngComm.*, **10**, 915 (2008); (b) X.H. Zhou, X.D. Du, G.N. Li, J.L. Zuo, X.Z. You. *Cryst. Growth Des.*, **9**, 4487 (2009).

[8] J.P. Zhang, Y.Y. Lin, X.C. Huang, X.M. Chen. *J. Am. Chem. Soc.*, **127**, 5495 (2005).

[9] G.M. Sheldrick. *SHELXL, Program for the Refinement of Crystal Structures*, University of Göttingen, Germany (1997).
[10] J.E.V. Babb, A.D. Burrow, R.W. Harrington, M.F. Mahon. *Polyhedron*, **22**, 673 (2003).
[11] (a) B. Chen, M. Eddaoudi, S.T. Hyde, M. O'Keeffe, O.M. Yaghi. *Science*, **291**, 1021 (2001); (b) X. Bu, N. Zhang, Y. Li, P. Feng. *J. Am. Chem. Soc.*, **125**, 6024 (2003).
[12] S.A. Bourne, J.J. Lu, B. Moulton, M.J. Zaworotko. *Chem. Commun.*, 861 (2001).
[13] W.L. Zhang, Y.Y. Liu, J.F. Ma, H. Jiang, J. Yang. *Polyhedron*, **27**, 3351 (2008).
[14] (a) X.M. Lu, Y.Y. Chen, P.Z. Li, Y.G. Bi, C. Yu, X.D. Shi, Z.X. Chi. *J. Coord. Chem.*, **63**, 3923 (2010) and references therein; (b) T.L. Hu, R.Q. Zou, J.R. Li, X.H. Bu. *Dalton Trans.*, 1302 (2008) and references therein.
[15] (a) H. Chang, M. Fu, X.J. Zhao, E.C. Yang. *J. Coord. Chem.*, **63**, 3551 (2010); (b) D. Feng, S.X. Liu, P. Sun, F.J. Ma, W. Zhang. *J. Coord. Chem.*, **63**, 1737 (2010); (c) S.S. Chen, J. Fan, T. Okarmura, M.S. Chen, Z. Su, W.Y. Sun, N. Ueyama. *Cryst. Growth Des.*, **10**, 812 (2010); (d) Z. Su, Y. Zhao, M. Chen, W.Y. Sun. *CrystEngComm*, **13**, 1539 (2011); (e) X.G. Liu, L.Y. Wang, X. Zhu, B.L. Li, Y. Zhang. *Cryst. Growth Des.*, **9**, 3997 (2009).
[16] J. Costa, R. Ruloff, L.S. Burai, L. Helm, A.E. Merbach. *J. Am. Chem. Soc.*, **127**, 5147 (2005).
[17] P.K. Chen, Y.X. Che, S.R. Batten, J.M. Zheng. *Inorg. Chem. Commun.*, **10**, 415 (2007).